Review Letter

THE NATURE OF ELECTRON TRANSFER AND ENERGY COUPLING REACTIONS

Britton CHANCE

Johnson Research Foundation, School of Medicine, University of Pennsylvania, Philadelphia, Pennsylvania 19104, USA

Received 6 April 1972

1. Introduction The aim of this paper is to designate pathways of electron flow and energy coupling that are consistent with available data on the nature of the electron transfer components, especially the kinetics and thermodynamics of their reactions. Recent developments of ideas and experimental observations concerning the respiratory chain raise significant problems on the nature of the interaction of the electron transfer components and on the mechanisms of electron transfer that achieve a maximal efficiency of energy coupling. This contribution considers this problem in terms of a respiratory chain that consists of a group of quasi-equipotential carriers interspersed with energy coupling components of alternating redox potentials, and outlines in detail the channeling of electrons through Site II in order to achieve this maximal efficiency of energy coupling.

1.1. *The respiratory chain and cytochrome* b

The concept of a respiratory chain based on the flow of electrons though a graded sequence of redox changes mediated by a continuous sequence of carriers was implicit in Keilin's classical studies [1]. In fig. 1, the three sites of energy coupling (Sites I, II and III*) are also the sites of action of inhibitors: at Site I, amytal and rotenone; at Site II, antimycin A and hydroxyquinoline-*N*-oxide; at Site III, cyanide, carbon monoxide and other terminal inhibitors [2–14]. Evidence for the compulsory nature of electron transfer through the carriers of the respiratory chain is based largely upon extraction–reconstitution procedures and inhibitor studies [1–4].

The identification of cytochromes with energy coupling had its origins in the behavior of cytochrome *b* in fragmented membrane preparations (submitochondrial particles). For example, cytochrome *b* kinetics in the non-phosphorylating Keilin and Hartree submitochondrial particles showed a wide variation in the response of cytochrome *b* when compared with the response in intact cells [4] or in isolated mitochondria [5, 6]. Aberrant properties of cytochrome *b* in the Keilin and Hartree preparation are its slow rate of reduction by succinate and, in the presence of antimycin A, the red shift of its absorption band, the acceleration of its reaction rate, and the phenomenon of cytochrome *b* reduction following cytochrome *c* oxidation [4, 6, 15]. Unusual properties of cytochrome *b* in intact and fragmented pigeon heart mitochondria have been identified by its responses to ATP, uncouplers, and ion gradients [16–18]. Uncoupling causes the oxidation of a species of cytochrome *b* absorbing at 555–556 nm at 77°K. More recent data show this cytochrome *b*, now termed b_T because of its role in energy transduction, to have a double α-band at 563 and 555 nm and β-bands at 535 and 528 nm at 77°K [19–21].

The phenomenon of cytochrome *b* reduction upon addition of ATP to anaerobic, coupled mitochondria involves a reversed flow of electrons at a significant, albeit slow, rate [22]. On this basis the redox control of the velocity and direction of electron flow was emphasized [23, 24]. Quantitative measurements of the relationship between the ATP/ADP·P_i ratio and the degree of alteration of the oxidation–reduction state of the various carriers, for example, cytochrome *c*, have also been carried out [22–24]. Variation of the ATP/ADP·P_i value from 10^1 to 10^3 M^{-1} at constant succinate/fumarate ratios has been found to

alter the ratio b_T^{3+}/b_T^{2+} from 7 to 0.07 [25]. Many approaches lead to the idea that energy spans of ∿15 kcal per mole, equivalent to ∿600 mV for the transfer of a pair of electrons, exist at the three energy-coupling sites of the chain [23, 24, 26] a conclusion requiring that in State 4 the respiratory chain is in quasi-equilibrium with ATP/ADP·P_i.

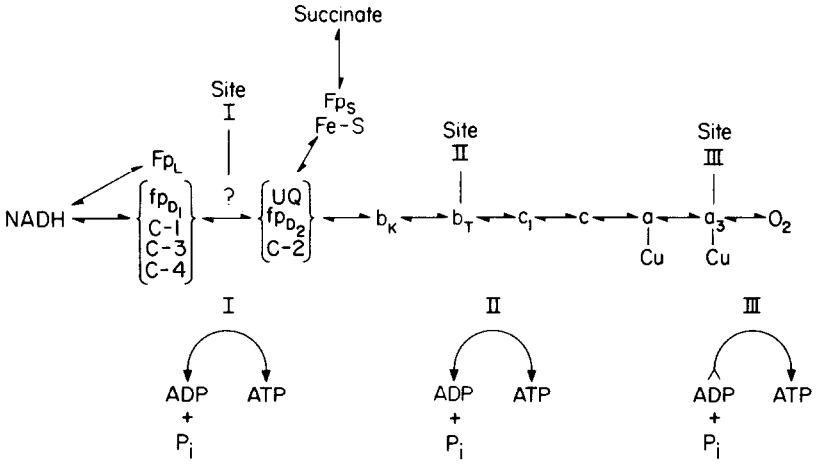

Fig. 1. The electron transfer components of the respiratory chain arranged as a continuous sequence from NADH (low potential) to oxygen (high potential). The components on the substrate side of Site I are Fp_L, the highly fluorescent lipoate dehydrogenase flavoprotein; fp_{D_1}, the NADH dehydrogenase flavoprotein, and iron–sulfur proteins here given as C-1, C-3, and C-4 [11]. On the oxygen side of Site I are Fp_S, the succinate dehydrogenase flavoprotein, with associated iron–sulfur proteins (Fe–S); UQ, ubiquinone; fp_{D_2}, the fluorescent flavoprotein; C-2 iron–sulfur protein; cytochromes b_K and b_T. On the oxygen side of Site II are the four cytochromes, c_1, c, a, and a_3, with associated copper [1–5; 8–12].

1.2. *Mid-potentials of cytochromes*

Consolidation and clarification of these viewpoints on the structure and function of the respiratory chain have been based upon significant developments in techniques for the in situ assay of the redox potential of its components. Initially devised for steady-state studies of photosynthetic systems [27–30] and for the study of cytochromes in mitochondria under aerobic conditions [31], these methods have recently been applied by Wilson and Dutton to the measurement of redox potential under anaerobic conditions [32, 33] and for the pulsed light activation of selectively poised photosynthetic systems [33–35]. The response of cytochromes b_T and a_3 to ATP can be quantitated as a shift of midpoint potential [36–38]; cytochrome b_T shifts in mid-potential from –30 mV in the de-energized state to +240 mV in the energized state, and cytochrome a_3 from over +400 mV to +190 mV.

A respiratory chain that intersperses three groups of electron carriers of fixed mid-potential (Groups I, II and III) with three energy-transducing carriers of variable potential is indicated in fig. 2. The diagram differs from that of fig. 1 in that the carriers are grouped thermodynamically. Two components – b_T at Site II and a_3 at Site III – are already identified to have ATP-dependent mid-potentials; a third such component will presumably be identified at Site I [9–12].

The function of the carriers in the fixed mid-potential Groups I, II and III is to serve as "redox potential buffer pools" and thereby fix the potentials between which the energy-transducing components operate. Thus, the respiratory chain operates at high thermodynamic efficiency by an energy transduction that proceeds through a series of quasi-equilibrium steps. Thus it is essential that oxidation–reduction reactions occur when the energy-transducing component, b_T, is quasi-equipotential with the appropriate group of electron carriers; for example, cytochrome

b_T in its low mid-potential form can react only with the Group II carriers and in its high mid-potential form, only with the group III carriers [39–41]. This communication identifies control and recognition mechanisms that channel the electron flow along the pathways of fig. 2 in order to achieve a high thermodynamic efficiency and a maximal energy conservation.

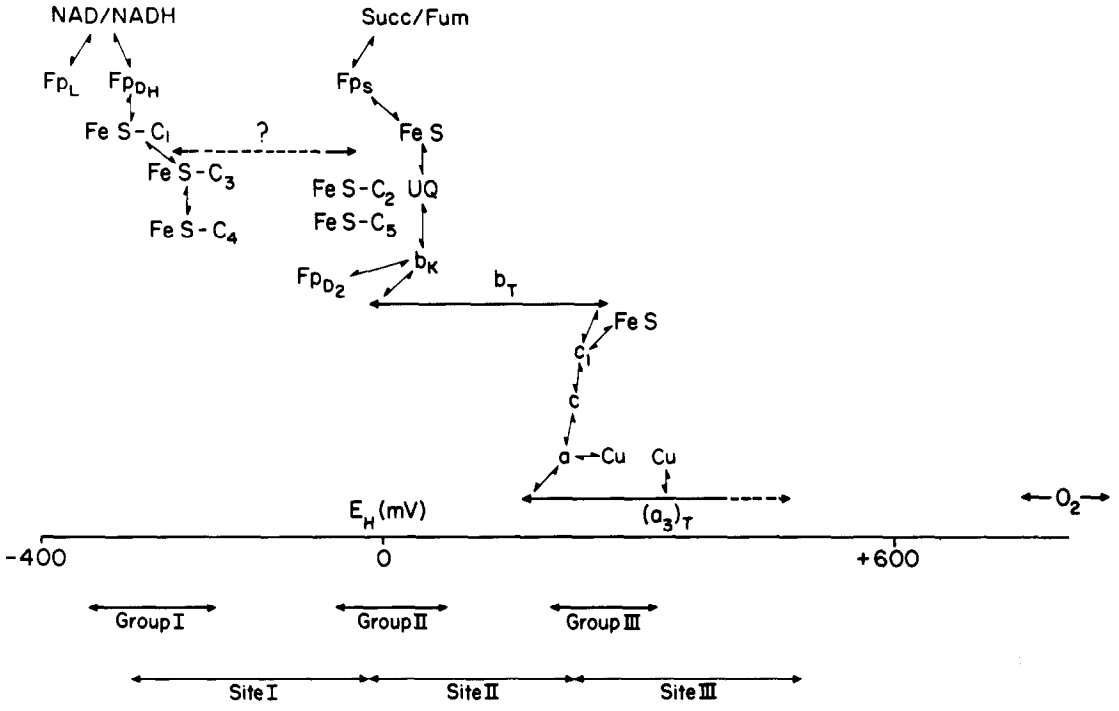

Fig. 2. The electron carriers of the respiratory chain arranged as groups of fixed potential (Groups I, II, and III) and individual components of variable mid-potential: cytochromes b_T and $(a_3)_T$ for Sites II and III and (?) for Site I. The other components are designated as in fig. 1 [36, 37, 47, 48, 77, 78].

2. Energy-dependent properties of cytochrome b_T

The high and low mid-potential forms of cytochrome b_T are considered appropriate to quasi-equilibrium reactions with the Group III and Group II carriers, respectively. Control of the rates of electron transfer is generally due to the distribution of the four species of cytochrome b_T: oxidized high mid-potential, b_{TH}^{3+}; oxidized low mid-potential, b_{TL}^{3+}; reduced high mid-potential, b_{TH}^{2+}; and reduced low mid-potential, b_{TL}^{2+}. Examples of the remarkable properties of cytochrome b_T kinetics in pigeon heart mitochondria are described here that illustrate electron flow patterns consistent with the various distributions of these four forms of this energy-transducing cytochrome in accord with the diagram of fig. 2.

2.1. *The energy-dependent kinetics of cytochrome* b_T

The kinetic properties of cytochrome b_T can be recorded by dual wavelength spectrophotometry in the rapid flow apparatus [19, 38]. The absorbancy contributions from the two types of cytochrome b – b_K of fixed mid-potential with an absorbancy maximum at 561 nm and b_T of variable mid-potential with an absorbancy maximum at 565 nm at 23° – are roughly 2:1 in favor of b_K at 560 nm and roughly 4:1 in favor of b_T at 566 nm.

In the experiment shown in fig. 3 the mitochondria are initially anaerobic and de-energized. They are poised at a potential rendered sufficiently negative by

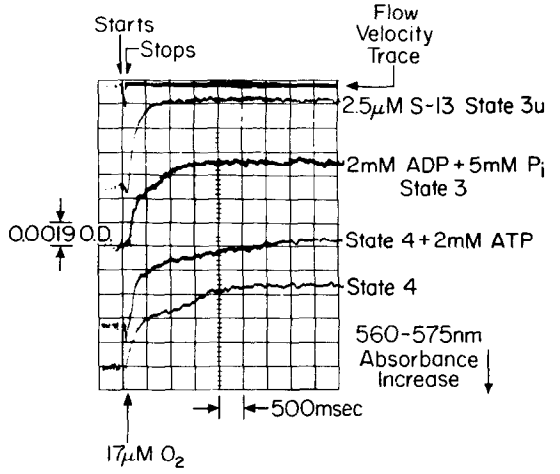

Fig. 3. The effect of ATP, ADP + P_i and an uncoupler, S-13 (5-chloro-3-t-butyl-2'-chloro-4'-nitrosalicylanilide) upon the oxidation kinetics of cytochromes b_K and b_T recorded in the regenerative flow apparatus. 2.8 mg of pigeon heart mitochondrial protein per ml, 6 mM succinate, glutamate, and malonate; after anaerobiosis is established, 5 μM rotenone is added [19].

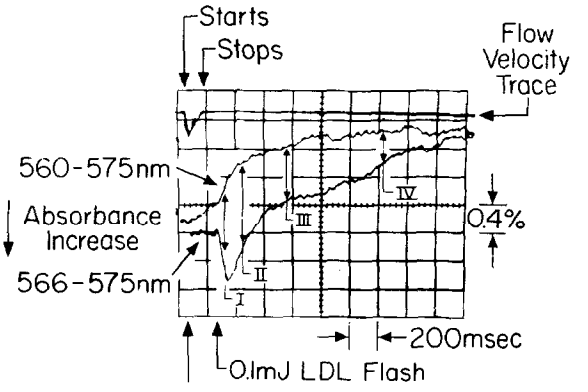

Fig. 4. The transient response of cytochromes b_T and b_K to laser flash photolysis of the cytochrome a_3:CO compound in the presence of 17 μM oxygen. 2.3 mg of pigeon heart mitochondrial protein per ml, suspended in 0.2 M mannitol, 0.03 M sucrose, 0.02 M MOPS (morpholinopropane sulfonate) buffer, pH 7.0, in the presence of 6 mM succinate, 6 mM malonate, 1.5 mM glutamate, 5 μM rotenone, and 600 μM carbon monoxide at 23°. The wavelength of the liquid dye laser flash is 585 nm. Time proceeds from left to right. Cytochrome b_T measured at 566–575 nm, b_K at 560–575 nm.

succinate plus glutamate to reduce cytochrome b_K completely and cytochrome b_T partially (cf. fig. 2). The moment of injection of oxygen is indicated on the top (flow velocity) trace, as is the time the flow stops. This pulse of oxygen, delivered in a few milliseconds by rapid mixing in the regenerative flow apparatus [19] causes an abrupt oxidation of cytochrome c_1 in about 20 msec and a rapid oxidation of cytochromes b_T and b_K in the first 100 msec of fig. 3 in the de-energized state. However, as the oxidation proceeds, the reaction slows as shown in the traces, to an increasing extent in the sequence from the uncoupled to the (ADP + P_i)-supplemented to the ATP-supplemented state. The fact that the ATP-supplemented rate is approached by that in State 4 in which no ATP has been added suggests that the mitochondria are energized to the same extent in the two cases. The small rapid phase in the initial stage of the combined cytochrome b_K–b_T kinetics even in the energized state is a complex phenomenon that is related to the tendency of cytochrome b_T to become reduced prior to its oxidation (cf. fig. 5). However, 200 msec after adding oxygen the reaction of b_T and c_1 represents an approach to equilibrium of quasi-equipotential carriers as in the scheme of fig. 2.

2.2. *Transient responses of cytochrome* b_T

The experiment of fig. 3 was designed to show the total response of cytochromes of type *b*, emphasizing their approach to the quasi-equilibrium state. The second unusual phenomenon of cytochrome b_T kinetics is revealed in two studies of the transient phases of the reaction, which show a rapid and brief shift of redox state in the direction opposite to that of the other carriers. In fig. 4, the two absorbing components of fig. 3, cytochromes b_K and b_T are time- and wavelength-resolved by rapid kinetic techniques. In fig. 5 the transient phase is prolonged by the depletion of cytochrome *c* and the cytochrome b_T–c_1 interaction is examined in detail.

This reverse transient in the cytochrome b_T kinetics was observed early in the study of yeast cells [15] which showed an uncoupler-insensitive oxidation of cytochrome *b* to occur in the aerobic–anaerobic transition in the antimycin A inhibited yeast cells. This reaction has been further studied by Kovac et al. [42]. Pumphrey [43] noted a similar effect in non-phosphorylating, detergent-clarified beef heart mitochondria, a phenomenon further investigated by Slater [44] and by Baum and Rieske [45, 46]. The experiments of this paper show that cytochrome b_T

reduction depends upon cytochrome c_1 oxidation; the phenomenon can be observed in coupled and uncoupled mitochondria, in the presence and absence of antimycin A, and is a general characteristic of the initiation of electron transport by oxygen pulses in anaerobic mitochondria [47, 48].

In fig. 4, the mitochondria slowly metabolize succinate and glutamate in the presence of malonate and rotenone; their reaction with oxygen is blocked by carbon monoxide. A pulse of oxygen delivered in the flow apparatus causes only small changes in b_T and b_K in the 120 msec interval between the stop of the flow and the laser flash which starts the reaction by photolyzing cytochrome a_3^{2+}:CO in the presence of oxygen. The Group III carriers are rapidly oxidized; the half-time for cytochrome c_1 is ∿7 msec.

Four phases of cytochrome b_T and b_K kinetics following the laser flash are illustrated. In Phase I, 30% of the total cytochrome b_T is reduced with a half-time of 7 msec (determined in experiments on a faster time scale, not shown here) and a peak of reduction is reached in 70 msec. A fast phase of b_K oxidation corresponds to the fast phase of b_T reduction, and suggests that cytochrome b_K is the electron donor to b_T, in agreement with the antimycin A insensitivity of this phase of the reaction (cf. fig. 5). After 70 msec, Phase II begins. Cytochrome b_T is oxidized at a rate roughly an order of magnitude slower than that of its reduction in Phase I, and there is a corresponding, slower phase in the oxidation kinetics of cytochrome b_K. At this time, cytochrome c_1 is acting as an effective electron acceptor for cytochrome b_T. A third phase begins 350 msec after the laser flash; cytochrome b_T and b_K continue to be oxidized in what is now a quasi-equilibrium reaction of b_{TH} with c_1 of the Group III carriers and b_{TL} with b_K of the Group II carriers, in accordance with the diagram of fig. 2. In Phase IV, after 1 sec, the rate of oxidation of b_T accelerates distinctly while that of b_K is not perceptibly altered, probably because the ubiquinone pool is oxidized by this time. In summary, there appears to be a complex transient response of cytochrome b_T consisting of an initial phase in which cytochrome b_K donates electrons to b_T and in which cytochrome c_1 does not yet appear to be able to accept electrons from b_T. In the second phase, the normal electron flow pathway is competent and rapid. In the third phase it is very slow and finally, in the fourth phase, a slight acceleration occurs.

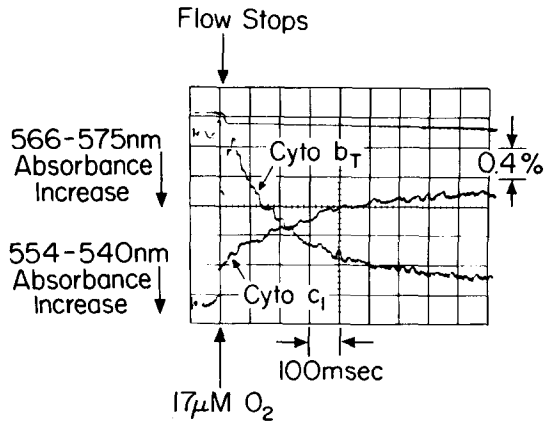

Fig. 5. A comparison of the kinetics of cytochrome c_1 oxidation (absorbance decrease at 554–540 nm) and cytochrome b_T reduction (absorbance increase at 566–575 nm) in oxygen pulse experiments. Conditions as in fig. 3, except that the mitochondria have been KCl-washed to deplete cytochrome c, and 0.15 μg of antimycin A per mg of protein is present [91].

The role of cytochrome c_1 in this reaction is identified in fig. 5, where removal of 80% of the cytochrome c delays the oxidation of cytochrome c_1 in response to the oxygen pulse. Furthermore, anticymin A has been added to ensure that cytochrome c_1 is not an effective electron acceptor in this reaction. Thus, the time sequence of events in Phase I is now spread out over a period of 1.0 sec, and can be observed readily without the need for laser flash photolysis; here the oxygen pulse is applied directly to the reduced carriers. After a brief transient in the cytochrome c_1 kinetics, the reduction of cytochrome b_T follows a course parallel to the oxidation of c_1. The antimycin A concentration in this experiment is so high that no perceptible oxidation of cytochrome b_T by forward electron flow occurs in the 0.9 sec interval of the recording.

One explanation [47, 48] for this reaction (for others, see sections 3.7 and 3.8 below) is that when the mitochondria are in the anaerobic, de-energized state, cytochrome b_T is in its low mid-potential form (b_{TL}) corresponding to the left-hand end of the arrow of fig. 2. Upon oxidation of cytochrome c_1, an interaction of cytochromes b_K and b_T occurs, converting cytochrome b_{TL} to b_{TH} (right-hand end of

arrow, fig. 2). While b_{TH} cannot be oxidized by c_1 because of the antimycin A block, it can readily be reduced by the Group II carriers since its mid-potential is now higher, instead of lower, than theirs. This interpretation suggests that transient phases of the electron flow pattern may not be in accord with the general postulate that oxidation–reduction reactions should occur when the energy-transducing component is quasi-equipotential with its oxidant or reductant.

2.3. *ATP-induced reversed electron flow*

The quantitative relationship between ATP/ADP·P_i and the oxidation of cytochrome c_1 and reduction of cytochrome b has been a topic of interest in this laboratory and in that of Klingenberg as well [22–24]. It has been found that the slope of the ATP/ADP·P_i titration of cytochrome b_T is negative, since b_T becomes more reduced with increasing ATP concentrations, responding sensitively to the phosphorylation potential; the midpoint of the titration corresponds to 30 M^{-1} ATP/ADP·P_i [49]. A titration of cytochrome c with ATP, ADP and P_i, on the other hand, has a slope of 0.5 and a mid-value for ATP/ADP·P_i of 10^4 M^{-1} [25]. The difference in behavior of cytochromes b_T and c_1 is emphasized in the data of this paper, and is consistent with the diagram of fig. 2, where b_T is shown to interact with ATP and to serve as the oxidant for the Group III carriers.

The key role of the high and low midpotential forms of cytochrome b_T in reversed electron flow is illustrated in fig. 6 by the nearly simultaneous oxidation of cytochrome c_1 of the Group III carriers and reduction of flavoprotein Fp_{D2} of the Group II carriers, verifying that ATP addition increases the concentration of b_{TH}^{3+} and b_{TL}^{2+}, thereby initiating reversed electron flow according to fig. 2 and fig. 7 below.

In this experiment, reduction of the three components – cytochrome c_1, fluorescent flavoprotein (Fp_{D2}) and cytochrome b_T (cf. fig. 2) – is indicated by a downward deflection of the traces. Electron transport from NADH-linked substrates is blocked by rotenone and since oxygen is present, the carriers are in the oxidized state prior to the start of the recording. Addition of sodium sulfide causes a nearly complete reduction of cytochrome c_1, due in part to

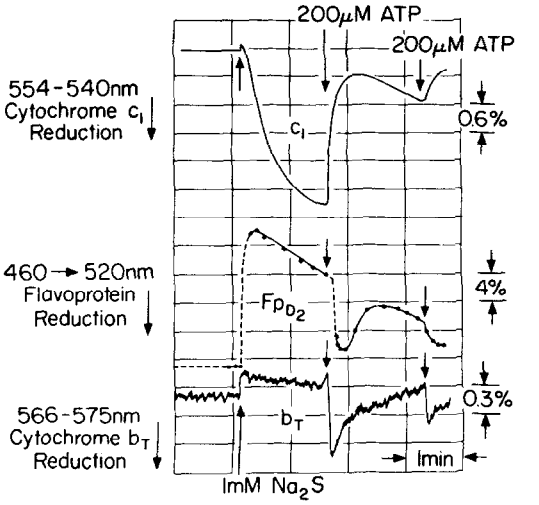

Fig. 6. An illustration of the operation of cytochrome b_T in reversed electron transport in pigeon heart mitochondria blocked with rotenone and sulfide so as to isolate Site II from Sites I and III. Approx. 3 mg of mitochondrial protein per ml, 0.25 M sucrose, 0.01 MOPS (morpholinopropane sulfonate) buffer, pH 7.2, 1.0 mM sodium sulfide, 200 μM ATP added at the point indicated in the diagram. Cytochrome c_1 measured spectrophotometrically at 554–540 nm, cytochrome b_T at 566–575 nm, in a rotating filter, four-wavelength apparatus in which flavoprotein fluorescence is excited at 460 nm and emission measured at 520 nm. Cytochromes c_1 and b_T are recorded simultaneously on the same strip chart; the flavoprotein trace was measured simultaneously and has been replotted from a separate chart. Temperature, 23°. Experiment in collaboration with A. Scarpâ.

endogenous substrate but also to the mild reducing effect of Na_2S [22]. The fluorescent flavoprotein makes a transition in the direction of oxidation, presumably because of the cessation of energy coupling via endogenous substrates (fatty acids) at the level of the Group II carriers. Cytochrome b_T shows a small and abrupt change in the direction of oxidation. Over the next 2 min, the system slowly seeks its new steady state, cytochrome c_1 reaching a plateau, cytochrome b_T remaining essentially constant, and Fp_{D2} drifting towards a somewhat more reduced state. At this point, ATP is added; Fp_{D2} and b_T are reduced and c_1 is oxidized. The abrupt reduction of cytochrome b_T suggests that the predominant effect of ATP is to raise the concentration of b_{TH}^{3+}, thereby activating the oxidation of c_1^{2+}:

$$b_{TH}^{3+} + c_1^{2+} \rightleftharpoons b_{TH}^{2+} + c_1^{3+} \quad (1)$$

In addition, the reaction of b_{TL}^{2+} with b_K^{3+} to form reduced Fp_{D2} is observed in the following net reaction:

$$2b_{TL}^{2+} + \text{ox } Fp_{D2} \rightleftharpoons 2b_{TL}^{3+} + \text{red } Fp_{D2}. \quad (2)$$

The latter reaction is suggested by the abrupt "turn-around" of the b_T trace 3 sec after the addition of ATP. The further trend of the Fp_{D2} trace in the direction of oxidation is possibly due to residual electron flow through the rotenone-blocked Site I, which we have not been able to inhibit completely at these low electron flow rates. It is for this reason that the principal interpretation must be placed upon the initial deflection of the traces immediately following ATP addition. During the next minute, cytochrome c_1 becomes less oxidized and b_T becomes less reduced. Evidence that this is due to a decrease of the ATP/ADP·P_i value is provided by the response to a second addition of ATP, which restores the initial oxidation of cytochrome c_1 and reduction of b_T and Fp_{D2}.

A more detailed analysis of the operation of cytochrome b_T in reversed electron transport is not possible because of the contributions of both b_{TH}^{2+} and b_{TL}^{2+} and a small (<20%) contribution of b_K^{2+} at 566–575 nm. Nevertheless, the data indicate that cytochrome b_T in the ATP-supplemented mitochondria under conditions where Site II is isolated from Sites I and III by rotenone and sulfide serves as an oxidant for the Group III carriers and a reductant for the Group II carriers in reversed electron transport, in accordance with fig. 2.

2.4. *Computer studies*

Computer simulation of the altered kinetics of cytochrome b_T permits an evaluation of the ratios of the forward and reverse velocity constants in the coupled and uncoupled states. No attempt has been made to distinguish the four species of cytochrome b_T; the results of the simulation simply identify the overall extent of the difference in the kinetic properties of b_T in the two states, and thereby give some indication of the magnitude of the difference in mid-potential between b_{TH} and b_{TL}. Reaction kinetics for the components c_1, b_K, b_T, and ubiquinone have been determined for the coupled and uncoupled pigeon heart mitochondria; the computer simulation then obtains "best fit" forward and reverse reaction velocity constants for the electron transfer reactions, assuming ubiquinone to be a one-electron carrier. A simplified explanation is that the ratios of these constants are the equilibrium constants between the carriers, and the ratios of the equilibrium constants correspond to the changes of mid-potential between the carriers in the coupled–uncoupled transitions. The change of kinetic constants is more than 5,000-fold, corresponding to an increase of mid-potential of more than 220 mV [50].

The validity of the mid-potential shifts observed in the Wilson–Dutton redox potential titrations has been questioned by one of the proponents of the methods [51] who found that a single mediator, vitamin K_5, showed a single species of cytochrome b in rat liver mitochondria, with an ATP-independent mid-potential of +75 mV, as compared with previous determinations of +40 in beef heart particles [52, 53]. It is probable that vitamin K_5 equilibrates with one of the Group II carriers of fixed potential (presumably cytochrome b_K) and that the multiple-mediator method [33] gives more useful results in electrometric titrations of mitochondria. Furthermore, all the data of figs. 3–6 and those for the computer simulations have been determined without the use of mediators, and therefore provide independent support for the shifts of mid-potential of cytochrome b_T. The consistency of the results from these several approaches seems impressive.

3. Control mechamisms

3.1. *Molecular basis*

With the data available on the nature of the respiratory chain from the thermodynamic standpoint, together with these examples of the characteristic responses of cytochrome b_T to control by the oxidation–reduction state of cytochrome c_1 and by ATP/ADP·P_i, it is appropriate to explore the possible molecular basis for these reactions. Two aspects of the reaction mechanism may be considered. First, the observation that ATP alters the mid-potential of the energy-transducing cytochrome finds its firm foundation in Mansfield Clark's pioneering studies [54] of the effect of heme liganding upon the oxidation–reduction potential [32, 33, 36, 37]. It is most

unlikely that ATP itself is the ligand of the heme; presumably, non-phosphorylated intermediates in ATP synthesis play this role.

Secondly, the observation that the oxidation–reduction state of cytochrome c_1 may control the mid-potential of cytochrome b_T has for its explanation the well-founded studies of heme-linked conformation changes in myoglobin and hemoglobin [55–58]. These results are linked to cytochrome function by the recent identification of tertiary structure changes in the oxidation–reduction reactions of cytochrome *c* [59].

This nature of the change in the heme environment was suggested by preliminary observations that indicated a correlation of the spin state of the iron atom of ferrimyoglobin with tertiary structure changes as indicated by two-dimensional Fourier difference syntheses [57, 58]. The striking changes in the three-dimensional structure of hemoglobin affords support in depth for this interpretation. The "out-of-plane, high-spin" iron is converted to "in-plane, low-spin" iron, with concomitant changes in protein structure, not only in the same [56] but also in adjacent portions [55] of the molecule. In cytochrome *c*, where only a small change of spin state occurs in the oxidation–reduction reaction, a considerable structural change is observed between the "open" structure of the oxidized cytochrome and the "closed" structure of the reduced molecule [59]. These models suggest that the redox reaction, coupled to the change of spin state and tertiary structure in one hemoprotein can transmit control signals to an adjacent hemoprotein, either as subunits of a single molecule or as closely interacting species – a phenomenon that may afford a mechanism for the interaction of cytochromes b_T and c_1 and ATP in the respiratory chain.

Such observations encourage the general view that changes in the heme environment of energy-transducing electron transfer components are linked to changes of tertiary or quaternary protein structure in an energy-conserving reaction. In the case of cytochrome b_T, the control of the heme environment via a change in the protein structure may occur either with the addition of ATP or with the oxidation of cytochrome c_1 thus affording an "elementary step" of energy conservation in the electron transfer chain of mitochondria.

3.2. *Hydrogen ions as a control mechanism*

Hydrogen ions may play a significant role at some energy-conserving sites, but not at others. One way to evaluate their role is to consider the effect of pH on the mid-potential of the cytochromes. For example, the mid-potential of cytochrome b_T shows a slope of less than 60 mV per pH unit in the range where oxidative phosphorylation occurs with maximal efficiency [60] and yet cytochrome a_3 shows a slope of very nearly 60 mV/pH unit [61]. In the case of cytochrome b_T, and possibly a_3 as well, the H^+-linked interactions between the heme environment and the protein structure may lead to changes in the pK's of imidazole and other groups and to redistributions of the charge on the molecules. For example, the slope of the redox potential titration for cytochrome b_T is consistent with a reduction of cytochrome b_T by OH^+ and an oxidation by OH^-. Such controls would readily operate in both directions; the change of the H^+ concentration could alter the heme environment and the redox potential, and thus be related to energy conservation [62–64]. In addition, the withdrawal of an electron from the heme of cytochrome c_1 in its oxidation alters its charge in relation to cytochrome b_T. This too may contribute to the interaction with cytochrome b_T ([65] and D. DeVault, personal communication). In this way, alterations of charge distribution in the energy-transducing electron transfer component may be a significant factor in controlling its reactivity and in modulating the changes of heme environment that are essential for energy coupling.

In the membrane-bound components, the linkage could extend to other proteins and lipids of the membrane structure, resulting in a "membrane Bohr Effect" [66] that leads to a transmembrane redistribution of charge. The direct contribution of electron transport to the membrane charge is difficult to determine; in intact mitochondria, Sites II and III generate less than 0.36 nmoles of H^+ per mg of protein in oxygen pulse experiments in which Ca^{2+} uptake is minimized [67]. This experiment, repeated with 10-fold greater sensitivity, now gives only 0.04 nmoles of H^+ per mg of protein (B. Chance and A. Scarpa, unpublished observations).

A recent paper suggests that respiratory control may be obtained in a reconstituted cytochrome oxidase–soy bean lipid structure [68]. Since these vesicles have the same structure as do mitochondria,

with cytochrome c outside, the following hydrogen atom transfer reaction takes place following cytochrome c oxidation by the membrane-bound oxidase:

$$AH_2 + 2c^{2+} \rightleftharpoons 2c^{3+} + A + 2H^+$$

In this reaction, external hydrogen ions are generated at Site III by the addition of external hydrogen donors. These vesicles provide an interesting model system, but have not yet shown ATP formation in the configuration that shows external H^+ formation. The preparation does show "respiratory control", but this phenomenon may be attributed to the internal alkalinization of the small vesicles [69] which is neutralized by the increased H^+ permeability induced by uncouplers. In addition, there is fairly strong evidence [70] against the existence, in the native membrane structure, of a hydrogen atom transfer of this type reducing the electron transfer components of Group III (cf. fig. 2).

The submitochondrial or inverted configurations of mitochondrial fragments bind $\sim$ 20 nmoles of H^+ per mg of protein [71] in a manner consistent with Mitchell's hypothesis [72] although the changes in H^+ concentration have not yet proved to be simultaneous with the oxidation of an identifiable hydrogen atom transfer component of the respiratory chain [73].

In summary, the magnitude of the structural changes at the level of the electron carriers and of the membrane is large enough so that considerable charge redistributions are to be expected in the energized, as compared with the de-energized, state. Such charge redistributions appear to be secondary consequences of the primary events in energy coupling that occur at the level of the heme environment of the energy-transducing cytochromes. Therefore, structural, conformational, and chemical mechanisms [70, 74–76] occurring at the molecular level will be described below.

3.3. *Control mechanisms at Site II*

In order to obtain maximal efficiency of energy coupling, electron flow must be channeled through quasi-equilibrium reactions of minimum potential gaps, and blocked across maximal ones, a restatement of the second law of thermodynamics that a reversible system gives maximal work [39]. This is a special problem at Site II since, as shown in fig. 2, in this region of the chain [8] there are up to three sets each of four species of electron transfer components, or a total of thirteen on both sides of the potential gap ([60–62, 77–79] and P.L. Dutton, personal communication). In order to ensure quasi-equipotential reactions, the oxidation of a low mid-potential form of cytochrome b_T by any one of the high potential cytochromes, or the reduction of high mid-potential b_T by a low-potential component such as b_K, ubiquinone, or flavoprotein [41, 60, 79] must be avoided. An acceptable model must meet these needs and also incorporate the available spectrophotometric, kinetic, and thermodynamic data on cytochrome b_T and on the Group II and III electron carriers. First, feasible pathways of electron transport in uncoupled preparations must be identified and second, constraints that appropriately channel electron flow for efficient energy conservation must be imposed. The diagram of fig. 7 indicates control mechanisms and electron flow pathways in a coupled system; the features of the mechanism are explained in detail in the following paragraphs.

3.4. *Formalism of the diagram*

The reaction mechanism is indicated as a rectangular sequence [41] in which the top and bottom lines represent the high and low mid-potential forms of the cytochromes and their left and right-hand sides the oxidized and reduced states, respectively. The components of the sequence consist of a minimum of three carriers: the cytochrome $b_T - c_1$ complex and its specific reductant, b_K. The valences "2+" or "H_2" indicate reduced forms. The high and low mid-potential values are indicated by the subscripts "H" and "L" respectively. Thus the typical configuration preceding Step 5 of fig. 7 is written: $b_K^{2+} b_{TH}^{3+} c_1^{2+}$.

Energy could be conserved in this redox cycle if the reduction of high mid-potential b_{TH}^{3+} by a low-potential carrier such as b_K or ubiquinone were avoided. Therefore, conformational alterations at the level of either the membrane or the molecular structures are proposed. The diagrams of fig. 7 are appropriate to both kinds of structural control: specific orientations of cytochromes b_T and c_1 are termed "proximal" (signified by a dot) or "distal" (signified by a cross) and hence competent or incompetent in electron transfer. In this notation, the configuration between Steps 4 and 5 of fig. 7 is written

$b_K^{2+} \times b_{TH}^{3+} \cdot c_1^{2+}$. The distal configuration prevents electron transfer across a wastefully large potential gap between b_{TH} and b_K; the proximal configuration permits quasi-equipotential electron transfer reactions

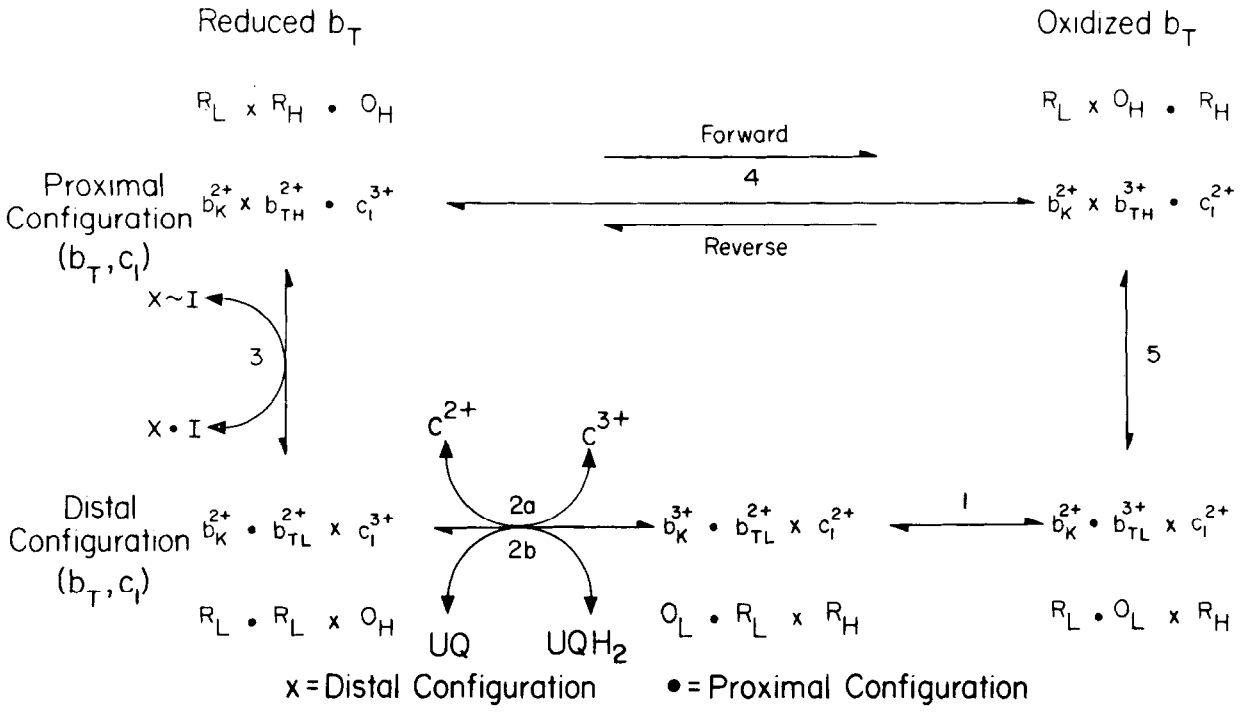

Fig. 7. An electron transfer pathway characteristic of energy conservation in steady-state electron flow in mitochondria, illustrating the essential structural constraints for efficient energy conservation.

of maximal energy-conserving efficiency to occur between b_{TH} and c_1. The two structures are in dynamic equilibrium, and the population of each configuration depends upon the heme environment or mid-potential of cytochrome b_T.

A simplified notation describing the b_K–b_T–c_1 interaction which affords a better overview of the key features of the reaction mechanism employs the letter "C" to indicate the three-cytochrome configuration; "R" and "O" indicate the oxidation–reduction state, and "L" and "H" again refer to the mid-potential values. Of the many possible configurations of these components, only a few are significant. The totality of relevant configurations for fig. 7 is represented by $^C(O/R)_L \cdot (O/R)_L \rightleftharpoons (O/R)_H \cdot (O/R)_H$, and appropriate derived configurations are discussed here. Proximal configurations capable of energy conservation by quasi-equilibrium electron flow correspond to the equilibration of b_{TL} with the Group II carriers, $^CR_L \cdot O_L \rightleftharpoons {}^CO_L \cdot R_L$, or of b_{TH} with the Group III carriers, $^CR_H \cdot O_H \rightleftharpoons {}^CO_H \cdot R_H$. The other configurations represent electron flow patterns leading to these configurations. The non-equipotential reaction discussed as possibly occurring in the transient phase of electron flow is $^CR_L \cdot O_H \rightleftharpoons {}^CO_L \cdot R_H$, corresponding to the reaction of b_{TL} with the Group III carriers.

3.5. *Reaction mechanisms for coupled systems: steady state electron flow*

The cyclic diagram of fig. 7 may be entered at Step 1 with a distal configuration of ferricytochrome b_T at −30 mV and ferrocytochrome c_1 at +220 mV: $b_K^{2+} \cdot b_{TL}^{3+} \times c_1^{2+}$. The mid-potential span between ferrocytochrome b_K at +30 mV and ferricytochrome b_T at −30 mV is small, and electron equilibration occurs between these two hemes in the first energy-conserving reaction, giving, in Step 1, $b_K^{3+} \cdot b_{TL}^{2+} \times c_1^{2+}$. At this point in the cycle, the hemes of b_K and c_1 are accessible to oxidation and reduction by the adjacent quasi-equipotential carriers of

Groups II and III, respectively, and an oxidation of c_1 by c and reduction of b_K and by ubiquinone or flavo-protein occurs in Step 2, to give $b_K^{2+} \cdot b_{TL}^{2+} \times c_1^{3+}$. The distal configuration prevents electron equilibration in an energy-wasting reaction between ferrocytochrome b_T at −30 mV and ferricytochrome c_1 at +220 mV. As cytochrome b_T shifts from low to high mid-potential in Step 3, using energy conserved in previous steps, the population of configurations shifts to give $b_K^{2+} \times b_{TH}^{2+} \cdot c_1^{3+}$, in which ferrocytochrome b_T and ferricytochrome c_1 have respective mid-potentials of +240 and +220 mV. The second quasi-equipotential energy-conserving redox reaction between these two carriers occurs in Step 4. The reaction product, $b_K^{2+} \times b_{TH}^{3+} \cdot c_1^{2+}$, contains a distal configuration of ferrocytochrome b_K at +30 mV and ferricytochrome b_T at +240 mV, and thereby avoids an energy-wasting reaction. Again, the population of configurations shifts as ferricytochrome b_T makes a transition to a low mid-potential form, $b_K^{2+} \cdot b_{TL}^{3+} \times c_1^{2+}$, in Step 5. At the same time, a proximal configuration of ferrocytochrome b_K and ferricytochrome b_T is permissible, since these two components are now quasi-equipotential. The cycle is now complete.

3.6. *Energy coupling*

Energy may be taken out of the cycle of fig. 7 to form ATP. Such reactions require either parallel pathways or two turns of the cycle to produce ATP, since redox titrations with mediators give a mid-potential shift of b_T of 275 mV, corresponding to only half the energy requirement for ATP formation [76]. Steps 3 and 5 are energy transfer steps in which chemical or structural mechanisms may function. Step 3 is identified as converting X·I, a low-energy intermediate, to X∿I, a high-energy intermediate [5, 7, 41] in which the energy is stored in a chemical or structural state. Step 3 seems to be a logical choice for this transition, since the State 4→3 transition which activates Step 3 would greatly increase the velocity of the $b_{TH}^{2+} \cdot c_1^{3+}$ reaction, and cause the cycle to run rapidly in the clockwise direction. In addition, a high ATP/ADP·P_i value in the absence of oxygen would cause the cycle to run counter-clockwise, leading to oxidation of the Group III carriers by a reversal of Steps 4 and 2a, and to reduction of the Group II carriers in Steps 1 and 2b.

3.7. *Transient responses: the energy-dissipating pathway*

The operation of a cycle involving quasi-equilibrium electron transfer reactions that is identical or very similar to the scheme of fig. 7 for the coupling of electron flow to energy conservation is assured from the chemical evidence for the high efficiency of ATP formation in oxygen reduction [76]. However, observations of the transient phases of cytochrome b_T reduction require consideration, and two categories of explanation are proposed. In the first case are those which are consistent with electron transfer across quasi-equipotential steps but inconsistent with experimental data; in the second case, those which are inconsistent with quasi-equipotential electron transfer but consistent with the experimental results on the transient interval, and provide as well transitions to the quasi-equipotential reactions of fig. 7.

The steps in Equation 3, representing the first case, are consistent with the diagram of fig. 7; the proximal configuration of $b_{TH} \cdot c_1$ resembles that between Steps 3 and 4, except that cytochrome c_1 is reduced. Oxidation of c_1 by c at this point leads to oxidation of b_{TH} in the energy-conserving reaction of Step 4, a transition of b_{TH} to b_{TL} in Step 5, and an energy-conserving oxidation–reduction reaction between b_K and b_T in Step 1 (compare [80]).

$$b_K^{2+} \times b_{TH}^{2+} \cdot c_1^{2+} \overset{c^{3+} \rightarrow c^{2+}}{\rightleftharpoons} b_K^{2+} \times b_{TH}^{2+} \cdot c_1^{3+} \overset{\text{Step 4}}{\rightleftharpoons} b_K^{2+} \times b_{TH}^{3+} \cdot c_1^{2+} \overset{\text{Step 5}}{\rightleftharpoons} b_K^{2+} \cdot b_{TL}^{3+} \times c_1^{2+} \overset{\text{Step 1}}{\rightleftharpoons} b_K^{3+} \cdot b_{TL}^{2+} \times c_1^{2+}. \quad (3)$$

This reaction requires the oxidation of b_{TH}^{2+} prior to its reduction in an antimycin A insensitive reaction; in more clearly defined terms, the reaction of b_{TL} with c_1 may be antimycin A sensitive, and that of b_{TH} with c_1 may not.

The bulk of the experimental evidence cited below is against this otherwise attractive scheme for maintaining the cytochromes of fig. 7 operative in the transient phases of electron transport. The experimental arguments are formidable:

1) The mid-potential of cytochrome b_{TL} is below, and that of b_{TH} is above, that of the succinate/fumarate couple prior to the oxygen pulse in de-

energized mitochondria, establishing the initial states as containing almost exclusively b_{TL}^{3+} and b_{TH}^{2+}.

2) Anticymin A blocks the oxidation of both b_{TL}^{2+} and b_{TH}^{2+} in the transient phase of 200 msec following the oxygen pulse but does not alter the rate of their reduction in the oxygen pulse response.

3) The reduction of cytochrome b_T is the primary electron transfer event; no prior oxidation of b_T or related effects upon c_1 oxidation are observed. The rate of b_T reduction in the transient phase is largely insensitive to uncouplers.

4) The half-time for b_T reduction is $\leqslant 7$ msec, closely approaching that for c_1 oxidation at 23°.

It is apparent that Equation 3 violates the experimental observations 2)–4). Therefore, the second explanation involving non-isopotential electron transfer reactions in the first 200 msec after the oxygen pulse, with subsequent transition to the quasi-equipotential pathways of fig. 7 requires consideration. In this case, the reaction sequence starts with the configuration between Steps 1 and 5:

$$b_K^{2+} \cdot b_{TL}^{3+} \times c_1^{2+} \overset{c^{3+}}{\rightleftharpoons} b_K^{2+} \cdot b_{TL}^{3+} \times c_1^{3+} \rightleftharpoons b_K^{2+} \cdot b_{TH}^{3+} \times c_1^{3+} \rightleftharpoons b_K^{3+} \cdot b_{TH}^{2+} \times c_1^{3+} \rightleftharpoons b_K^{3+} \times b_{TH}^{2+} \cdot c_1^{3+}. \quad (4)$$

The oxygen pulse oxidizes cytochrome c_1 and, by means of a control of the environment of the heme of b_T exerted by the change in redox state of c_1, described in detail below, cytochrome b_{TL}^{3+} makes the transition to b_{TH}^{3+}, essentially the reverse of Step 5; however, the proximal relationship of b_K^{2+} and b_{TH}^{3+} is retained and a non-isopotential electron transfer occurs between these two carriers, giving a configuration that can rearrange to that between Steps 3 and 4. b_K^{3+} is reduced by endogenous substrate and the pathway of fig. 7 can then be followed.

A further possibility is based upon control of the configuration of b_K and b_T by the oxidation–reduction state of c_1. The initial state of the anaerobic mitochondria prior to the oxygen pulse would be that between Steps 4 and 5, with a distal $b_K - b_T$ configuration: $b_K^{2+} \times b_{TH}^{3+} \cdot c_1^{2+}$. Oxidation of cytochrome c_1^{2+} by the oxygen pulse, with a simultaneous transition to a proximal configuration between b_K and b_{TH} would lead to a rapid reduction of b_{TH} by b_K and a rearrangement to the configuration between Steps 3 and 4 of fig. 7, suitable for entering the cycle

$$b_K^{2+} \times b_{TH}^{3+} \cdot c_1^{2+} \overset{c^{3+} \rightarrow c^{2+}}{\rightleftharpoons} b_K^{2+} \cdot b_{TH}^{3+} \times c_1^{3+} \rightleftharpoons b_K^{3+} \cdot b_{TH}^{2+} \times c_1^{3+} \rightleftharpoons b_K^{3+} \times b_{TH}^{2+} \cdot c_1^{3+}. \quad (5)$$

While the first observation above indicates that prior to the oxygen pulse the presence of b_{TH}^{3+} is unlikely, the distal configuration of b_K and b_T in Equation 5 may render this observation inapplicable. Thus the two concepts – the control of the heme environment expressed in Equation 4 and the control of the cytochrome configuration expressed in Equation 5 – are closely related approaches to the control of the reactivity of cytochrome b_T by cytochrome c_1.

3.8. *Transition to energy-conserving pathways*

The acquisition of an energy-conserving configuration appropriate to quasi-equipotential electron transfer seems to occur within 200 msec after the oxygen pulse. In fig. 4, the reduction of cytochrome b_T is followed by an abrupt oxidation, even in mitochondria in which energy dissipation is blocked. However, the extent of the oxidation is no greater than that of the previous reduction. The subsequent kinetics are slow, suggesting that the energy-conserving configuration is established when or shortly after the reduction is maximal, In the case of Equations 4 and 5, the configuration of the reaction product is $b_K^{3+} \times b_{TH}^{2+} \cdot c_1^{3+}$, an energy-conserving configuration that is an appropriate point of entry into the sequence of fig. 7, preceding Step 4.

A similar transition may be involved in reactions with reductants. For example, durohydroquinone (H_2DQ) at a potential of +19 mV reduces cytochrome b_T slowly in the uncoupled state and very rapidly in the ATP-supplemented state [81]. The response observed in the presence of ATP is:

$$b_K^{3+} b_{TH}^{3+} c_1^{3+} \overset{H_2DQ}{\rightleftharpoons} b_K^{2+} b_{TH}^{2+} c_1^{2+}, \quad (6)$$

where durohydroquinone reduces b_{TH}^{3+} and c_1^{3+} directly or through b_K. Nevertheless, steady-state phosphorylation with durohydroquinone gives a P/O value of 2 [82]. It is apparent that electron flow in the steady state through the pathway of Equation 6 is

blocked by an appropriate distal configuration:

$$b_K^{3+} \times b_{TH}^{3+} \cdot c_1^{3+} \overset{H_2DQ}{\rightleftharpoons} b_K^{2+} \times b_{TH}^{3+} \cdot c_1^{2+}. \quad (7)$$

In summary, energy-dissipating configurations observed in the transient state may lead to the formation of energy-conserving configurations that persist in steady-state electron transfer. At this point, it is appropriate to consider model systems which provide a basis for the control by the heme environment and by the proximal and distal configurations of the respiratory carriers.

3.9. *Control mechanisms at the macromolecular level*

Electron flow in the proximal and distal configurations of fig. 7 is regulated by the restricted area of the cytochrome surface available for electron transfer and by the relative positions of the cytochromes. Control of electron flow through cytochromes *c* and *a* has been discussed in detail [70] and the mechanism identified in Scheme 5 of that paper applies here (cf. fig. 8) in the context of cytochromes b_T and c_1, the general idea being that juxtaposed or proximal hemes can readily transfer electrons while opposed or distal hemes cannot.

3.10. *The active region for electron transfer*

Evidence supporting a restricted active region of cytochrome *c* was first suggested by the molecular statistics of its oxidation by yeast cytochrome *c* peroxidase [83, 84] and more recently by studies of its reaction with hydrated electrons [85]. The size of the active region has now been identified by the X-ray crystal structure of the molecule [59] and by NMR measurements of electron delocalization [86]. From the kinetic and structural studies, the active region for electron transfer approximates the projection of the heme at the surface of the protein. Tunneling of electrons is depicted in fig. 8 as a possible control mechanism. Due to the exponential nature of the rate equation, a small change of the tunneling barrier width would cause a large change in the electrion transfer rate [70]. For this reason, the change from proximal and distal configurations for tunneling-limited electron transfer would not require large distance changes.

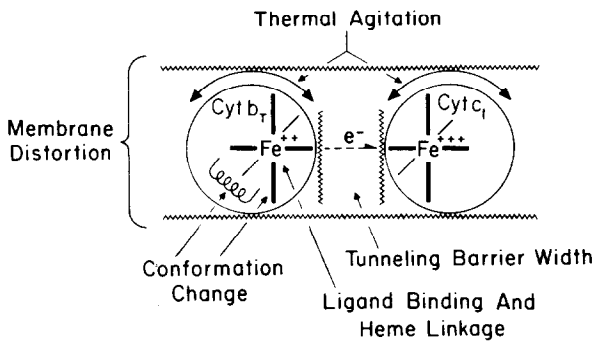

Fig. 8. A schematic diagram representing possible mechanisms for electron transfer between cytochromes [70].

3.11. *Mobility in membrane structures*

Variations of the relative positions of the cytochromes appropriate to distal and proximal configurations is made possible by their rapid rotational motions. Initially, we made the assumption that the rotational relaxation times of proteins in solution would apply to the membrane-bound proteins [4]. Mobility of cytochromes seems an essential feature of electron transfer through a sequence of carriers whose active site represents a small fraction of the total surface area; juxtapositions of the heme of each with that of its neighbors from time to time seems essential, and is exemplified in the diagram of fig. 8 [70].

The following experimental observations support the concept of rotational and translational mobility of cytochromes in membranes. First, spin-labelling of cytochrome *c* suggests an interaction of the methionine-65 site with the membrane structure and nevertheless a small immobilization in the vicinity of the probe [87, 88]. Secondly, observations of the movement of membrane components from one part of a fused animal cell to another give a high mobility in the plane of the membrane: 10^{-3} to 10^{-4} of that of a large protein in water [89, 90]. Thirdly, branching of electron flow from an uninhibited chain to one terminally inhibited with carbon monoxide is due largely to the mobility of cytochrome *c* from one group of carriers to another [91–94]. Fourthly, rhodopsin, a lipoprotein of molecular weight 40,000, is capable of fast rotational diffusion ($\sim$20 μsec) in the retinal membrane at 20° [95, 96]. Thus, the mobility of the cytochromes appears to be adequate to establish the distal and proximal configurations of fig. 7. In fact,

one might expect the configurations to be in rapid equilibrium [47, 48, 69].

Appropriate control of the populations of distal and proximal configurations and thus of the electron transfer according to the mid-potential value of cytochrome b_T is required. Control by membrane distortion is among the possibilities previously discussed [70] and in included in fig. 8. One approach postulates that the membrane phospholipids, either as individual components or as portions of the membrane structure, act to control the distal/proximal populations. As an example, oxidized cytochrome *c* has an open channel leading to the heme on the histidine-80 side, while reduced cytochrome *c* has a closed channel [59, 97]. In fact, the mid-potential of this cytochrome is altered in the presence of phospholipid [98]. We may propose that anchoring of cytochrome *c* to the lipid *via* this channel could be different in the oxidized and reduced states.

A second example of redox control by the localization of a membrane component is afforded by studies of the interaction of ubiquinone with the fluorescent probe AS (12-(9-anthroyl) stearic acid) in mitochondrial membranes ([99, 100] and unpublished observations with M. Erecinska and G.K. Radda). Oxidized ubiquinone is in rapid collision ($\sim 2 \times 10^8$ sec^{-1}) with the anthroyl group that is 14 Å inside the hydrocarbon region of the membrane. Yet reduced ubiquinone exhibits no significant collisional interaction with the probe, suggesting that the oxidized and reduced states of ubiquinone occupy different regions of the membrane, and that the membrane structure may be altered thereby.

An elucidation of this observation is afforded by low-angle X-ray diffraction studies [101] of dipalmitoyl lecithin bilayers occupied by oxidized or reduced ubiquinone. The oxidized form induces a statistically disordered amorphous packing. Reduction of ubiquinone leads to the formation of a somewhat disordered hexagonal lattice oriented normal to the plane of the bilayer. In this respect, the oxidation–reduction state of a model electron carrier controls the packing of the lipid chains in a model membrane. Assuming that these two examples are applicable to cytochrome b_T, it appears reasonable to speculate that the high and low mid-potential forms of the cytochrome would interact with the membrane structure so as to favor appropriate populations of distal or proximal configurations, as is illustrated in the mechanism of fig. 7.

3.12. *Heme iron – protein structure interaction*

While these considerations provide control of the configurations of cytochromes b_K, b_T and c_1 in the cycle of fig. 7, an additional control appears to be exercised over the mid-potential of cytochrome b_T by the oxidation–reduction state of cytochrome c_1, as in the traces of figs. 4 and 5. Here, ligand binding, heme linkage, and conformation change in fig. 8 are based upon current views on cooperative mechanisms in oxygen-binding hemoproteins [55–58]. The change of liganding at the sixth coordination position of ferrous hemoglobin causes a transition to the low-spin diamagnetic oxyhemoglobin with the heme atom in the heme plane, evoking structural controls through the heme linkages such as the F-8 histidine to various parts of the subunits of the molecules, particularly the interface between subunits of the tetramer, and to the hemes of other subunits, thus altering their structure and reactivity [55].

In cytochromes b_T and c_1, both heme iron atoms are six-coordinated to the protein, and the simple idea of ligand control of the spin state and structure is inapplicable. Instead, structure changes in b_T may be generated by spin-state or structure changes of the heme of cytochrome c_1 induced by changes in its oxidation–reduction state. While these spin-state changes are small in cytochrome *c*, they nevertheless seem large enough to cause a general transformation of the protein structure from a relatively open configuration to a closed configuration in the vicinity of the heme [59, 97] with appropriate alterations in heme–heme interaction. Assuming that analogous changes of cytochromes c_1 and b_T occur in the oxidation–reduction cycle, the structural control of the heme environment of cytochrome b_T by the redox state of cytochrome c_1 could be transmitted by contact interaction of the two hemoproteins, as in the subunits of tetrameric hemoglobin. The action of cytochrome c_1 upon cytochrome b_T would also be expected to cause different relationships between the two cytochromes and thus to contribute to the control of the populations of the distal/proximal configurations as well (see p. 20, note b).

3.13. *Role of the uncoupler*

Equations 4 and 5 above identify uncoupled electron flow via an energy-dissipating electron transfer pathway. Suitable control mechanisms subsequently operate to enforce an energy-conserving pathway. An uncoupler could cause such control mechanisms to be ineffective and thus stabilize the energy-dissipating pathway. However, other alternatives are more likely. First, the uncoupler may act upon the energy-conserving pathway of fig. 7 simply by accelerating the transitions between b_{TL} and b_{TH}, so that the reaction kinetics of cytochrome b_T in response to an oxygen pulse are accelerated. Secondly, explanations for uncoupler action based upon increased proton conductivity of the membrane [72] seem appropriate, and would similarly increase energy dissipation through ion transport systems. However, an inconsistency between this property as exhibited in model systems and the actual uncoupling of oxidative phosphorylation in intact mitochondria has been reported [102]. Recent data suggest that the uncoupler acts directly upon the purified ATP synthetase [103].

3.14. *Control mechanisms in transmembrane structures*

A further dimension of control could be afforded if there were asymmetric distributions of electron carriers of adjacent groups (I, II, and III) with respect to the hydrocarbon chains of the lipid components, with the energy-transducing components affording a trans-membrane shuttle. The model resembles that of Mitchell [72, 104] except that the energy-transducing cytochromes would be required to "shuttle" but would not be required to be hydrogen atom transfer components. A number of inconsistencies immediately arise, since ubiquinone would appear to afford superior qualities to cytochrome b_T as a transmembrane shuttle, and yet ubiquinone does not show the energy-dependent characteristics of cytochrome b_T recorded in figs. 3–6. Also, the very real problem of the transmission of control signals across the membrane remains unsolved and improbable; for example, oxidation of cytochrome c_1 on the outside of the mitochondrial membrane should transmit control information on its heme environment to b_T on the other side of the membrane. Lastly, such a mechanism would not be expected to operate in the purified b_T–c_1 complex [45–48, 105].

3.15. *Size of the interacting unit*

In the diagrams presented here, the interacting unit includes cytochromes c_1, b_T and b_K. There may be present a third type of cytochrome b as well ([76] and P.L. Dutton, personal communication). The necessity for these components in the cytochrome b_T–c_1 interaction may be evaluated from the results of extraction procedures. Ubiquinone may be extensively extracted and although the kinetics of the cytochrome b_T–c_1 interaction are affected because of the need for UQH_2 as electron donor, the reaction itself seems independent of the presence of ubiquinone [48]. Cytochrome b_K can apparently be largely removed [105] leaving a fraction which shows absorption bands characteristic of cytochromes b_T and c_1. While these fractions have not yet been tested for the kinetics of interaction of the two species, they appear to be active in reconstituting the electron flow from succinate to cytochrome c [105]. It seems, therefore that the reactive intermediate is at least as large as a dimer composed of cytochromes b_T and c_1 (see p. 20, note a).

3.16. *Relationship to current theories of oxidative phosphorylation*

The cycles identified here represent feasible pathways of electron transfer with high energy coupling efficiency achieved by reactions that are quasi-equipotential, i.e., of minimal ΔG. Thus, the intermediates of the cycle will be "charged" with an energy equivalent to one-half that required for ATP formation; two turns of the cycle, or parallel pathways, are required to conserve the full 600 mV for ATP formation. A specific high energy intermediate [3, 76, 106] such as $b\sim I$ is similar to b_{TH} and control of electron flow in State 4 is explained by its slow reaction rate and unfavorable equilibrium with cytochrome c_1. Energy coupling from the redox potential transitions of the mechanism of fig. 7 to the ATP synthetase may occur through chemical intermediates [41, 75, 76, 107] by structural changes [108] or both [109]. The former case involves the high-energy chemical configurations $X\sim I$ and $X\sim P$ which can be obtained by interaction with the heme environment directly [107] or through thiol or related compounds [75, 107, 110]. The latter case may involve a direct structural coupling between the structural changes at the level of the heme iron and the synthetase, as sug-

gested by changes of tritium-labeling in energy-coupling reactions of chloroplasts [111]. Thus, the configurations of cytochrome b_T-c_1 in Steps 3–5 of fig. 7 would interact structurally with the ATP synthetase molecule.

Transmembrane H^+ gradients may also contribute to energy conservation as Bohr effects across the molecules [66] of figs. 7 and 8 or across the membrane [104]. A chemiosmotic energy conservation reaction involving charge separation across the membrane dielectric [70, 104] may be of secondary importance; molecular interactions of the electron carriers afford the basis for the hypothesis presented here. These considerations focus attention upon the heme environment rather than the transmembrane proton gradient as the seat of energy conservation in the cytochrome chain.

Acknowledgements

This review has relied heavily upon frequent consultation with several colleagues, especially D. DeVault, P.L. Dutton, D.F. Wilson and M. Erecinska. Figs. 4 and 5 show unpublished experiments with M. Erecinska and fig. 6 with A. Scarpa, to whom many thanks are due. This research has been supported by USPHS GM 12202.

References

[1] D. Keilin, Proc. Roy. Soc. B-98 (1925) 312.
[2] A.L. Lehninger, in: Harvey Lectures, Series XIL, 1953–54 (Academic Press, New York, 1955) p. 176.
[3] E.C. Slater, Nature 172 (1953) 975.
[4] B. Chance, Nature 169 (1952) 215.
[5] B. Chance and G.R. Williams, J. Biol. Chem. 217 (1955) 409.
[6] B. Chance, J. Biol. Chem. 233 (1958) 1223.
[7] B. Chance and G.R. Williams, J. Biol. Chem. 217 (1955) 395.
[8] B. Chance, A. Azzi, I.Y. Lee, C.P. Lee and L. Mela, in: Mitochondria: Structure and Function, FEBS Symposia 17, eds. L. Ernster and Z. Drahota (Academic Press, London, 1969) p. 233.
[9] T. Ohnishi, D.F. Wilson, T. Asakura and B. Chance, Biochem. Biophys. Res. Commun. 46 (1972) 1631.
[10] T. Ohnishi, T. Asakura, T. Yonetani and B. Chance, J. Biol. Chem. 246 (1971) 5960.
[11] N.R. Orme-Johnson, N.H. Orme-Johnson, R.E. Hansen, H. Beinert and Y. Hatefi, Biochem. Biophys. Res. Commun. 44 (1971) 446.
[12] P.J. Albracht and E.C. Slater, Biochim. Biophys. Acta 245 (1971) 503.
[13] B. Chance, W. Holmes, J. Higgins and C.M. Connelly, Nature 182 (1958) 1.
[14] B. Chance, C.P. Lee, I.Y. Lee, T. Ohnishi and J. Higgins, in: Electron Transport and Energy Conservation, eds. J.M. Tager, S. Papa, E. Quagliariello and E.C. Slater (Adriatica Editrice, Bari, 1970) p. 29.
[15] B. Chance, Abstracts, II Intern. Congr. Biochem., Paris, 1952, p. 32.
[16] B. Chance and B. Schoener, J. Biol. Chem. 241 (1966) 4567.
[17] B. Chance, C.P. Lee and B. Schoener, J. Biol. Chem. 241 (1966) 4574.
[18] B. Chance and B. Schoener, J. Biol. Chem. 241 (1966) 4577.
[19] B. Chance, D.F. Wilson, P.L. Dutton and M. Erecinska, Proc. Natl. Acad. Sci. U.S. 66 (1970) 1175.
[20] N. Sato, D.F. Wilson and B. Chance, FEBS Letters 15 (1971) 209.
[21] N. Sato, T. Ohnishi and B. Chance, in preparation.
[22] B. Chance, J. Biol. Chem. 234 (1961) 1544.
[23] M. Klingenberg and P. Schollmeyer, Biochem. Z. 335 (1961) 243.
[24] M. Klingenberg and P. Schollmeyer, Biochem. Z. 335 (1961) 263.
[25] B. Chance, in: Biological Structure and Function, Proceedings, First Intern. Congr. Biophysics, 1960, eds. T.R. Goodwin and O. Lindberg (Academic Press, London, 1961) p. 119.
[26] E.C. Slater, in: Electron Transport and Energy Conservation, eds. J.M. Tager, S. Papa, E. Quagliariello and E.C. Slater (Adriatica Editrice, Bari, 1970) p. 363.
[27] I.D. Kuntz, P.A. Loach and M. Calvin, Biophys. J. 4 (1964) 227.
[28] M.A. Cusanovitch, R.G. Bartsch and M.D. Kamen, Biochim. Biophys. Acta 153 (1968) 397.
[29] W.A. Cramer and W. Butler, Biochim. Biophys. Acta 172 (1969) 503.
[30] H.N. Fan and W.A. Cramer, Biochim. Biophys. Acta 216 (1970) 200.
[31] A.H. Caswell, J. Biol. Chem. 243 (1968) 5827.
[32] P.L. Dutton, D.F. Wilson and C.P. Lee, Biochemistry 9 (1970) 5077.
[33] P.L. Dutton, Biochim. Biophys. Acta 226 (1971) 63.
[34] P.L. Dutton, T. Kihara, J.A. McCray and J.P. Thornber, Biochim. Biophys. Acta 226 (1971) 81.
[35] P.L. Dutton and J.B. Jackson, European J. Biochem., in press.
[36] D.F. Wilson and P.L. Dutton, Biochem. Biophys. Res. Commun. 39 (1970) 59.
[37] D.F. Wilson and P.L. Dutton, Arch. Biochem. Biophys. 136 (1970) 583.
[38] B. Chance, M. Erecinska, D.F. Wilson and P.L. Dutton, in: Energy Transduction in Respiration and Photo-

synthesis, eds. E. Quagliariello and S. Papa (Adriatica Editrice, Bari, 1971) p. 3.
[39] A.A. Noyes and M.S. Sherrill, A Course of Study in Chemical Principles (Mcmillan, New York, 1934).
[40] D. DeVault, in: Structure and Function of Cytochromes, eds. K. Okunuki, I. Sekuzu and M. Kamen (University Park Press, Baltimore, 1969) p. 488.
[41] D. DeVault, Biochim. Biophys. Acta 225 (1971) 193.
[42] L. Kovac, P. Smigan, E. Hrusovke and B. Hess, Arch. Biochem. Biophys. 139 (1970) 370.
[43] A. Pumphrey, J. Biol. Chem. 237 (1962) 238.
[44] E.C. Slater and J.P. Colpa-Boonstra, in: Haematin Enzymes, eds. J.E. Falk, R. Lemberg and R.K. Morton (Pergamon Press, Oxford, 1961) p. 575.
[45] J.S. Rieske, Arch. Biochem. Biophys. 145 (1971) 179.
[46] H. Baum, J.S. Rieske, H.I. Silman and S.H. Lipton, Proc. Natl. Acad. Sci. U.S. 57 (1967) 798.
[47] D.F. Wilson, M.C. Koppelman, M. Erecinska and P.L. Dutton, Biochem. Biophys. Res. Commun. 44 (1971) 759.
[48] M. Erecinska, B. Chance, D.F. Wilson and P.L. Dutton, Proc. Natl. Acad. Sci. U.S. 69 (1972) 50.
[49] N. Sato, Federation Proc. 30 (1971) 1190Abs (#801).
[50] M. Wagner, B. Chance and M. Erecinska, in: Energy Transduction in Respiration and Photosynthesis, eds. E. Quagliariello and S. Papa (Adriatica Editrice, Bari, 1971) p. 17.
[51] A.H. Caswell, Arch. Biochem. Biophys. 144 (1971) 445.
[52] F.A. Holton and J.P. Colpa-Boonstra, Biochem. J. 76 (1960) 179.
[53] P.F. Urban and M. Klingenberg, European J. Biochem. 9 (1969) 519.
[54] W.M. Clark, Oxidation–Reduction Potentials of Organic Systems (Waverly Press, Baltimore, 1960).
[55] M.H. Perutz, Nature 228 (1970) 726.
[56] R. Huber, O. Epp and H. Formanek, J. Mol. Biol. 52 (1970) 349.
[57] H.C. Watson and B. Chance, in: Hemes and Hemoproteins, eds. B. Chance, R.W. Estabrook and T. Yonetani (Academic Press, New York, 1966) p. 151.
[58] B. Chance, in: Probes of Structure and Function of Macromolecules and Membranes, Vol. II., eds. B. Chance, T. Yonetani and A.S. Mildvan (Academic Press, New York, 1971) p. 321.
[59] R.E. Dickerson, T. Takano, R. Sloanson and O.B. Kallai, Cold Spring Harbor Symposia Proceedings (1971) in press.
[60] D.F. Wilson, M. Erecinska, J.S. Leigh and M.C. Koppelman, Arch. Biochem. Biophys. submitted.
[61] D.F. Wilson, J.S. Leigh and J.G. Lindsay, Second Intern. Symposium on Oxidases and Related Redox Systems, eds. T.E. King, H.S. Mason and M. Morrison (John Wiley and Sons, New York) in press.
[62] M.K.F. Wikström, in: Proceedings, Intern. Symposium on the Biochemistry and Biophysics of Mitochondrial Membranes (Bressanone, Italy, 1971) in press.
[63] R.J.P. Williams, Current Topics in Bioenergetics 3 (1969) 79.
[64] A. Azzi, Biochem. Biophys. Res. Commun. 37 (1969) 254.
[65] J.B. Chappell, in: Proceedings, Intern. Symposium on Biochemistry and Biophysics of Mitochondrial Membranes (Bressanone, Italy, 1971) in press.
[66] B. Chance, A.R. Crofts, M. Nishimura and B. Price, European J. Biochem. 13 (1970) 364.
[67] B. Chance and L. Mela, Nature 212 (1966) 372.
[68] P.C. Hinkle, J.J. Kim and E. Racker, J. Biol. Chem. 247 (1972) 1338.
[69] B. Chance, in: Molecular Basis of Electron Transport, ed. J. Schultz (Academic Press, New York) in press.
[70] B. Chance, Biochem. J. 103 (1967) 1.
[71] S. Papa, F. Guerreri, M. Lorusso and E. Quagliariello, FEBS Letters 10 (1970) 295.
[72] P. Mitchell, Biol. Revs. 41 (1961) 445.
[73] B. Chance, G.K. Radda and C.P. Lee, in: Electron Transport and Energy Conservation, eds. J.M. Tager, S. Papa, E. Quagliariello and E.C. Slater (Adriatica Editrice, Bari, 1970) p. 557.
[74] B. Chance, C.P. Lee and L. Mela, Federation Proc. 26 (1967) 1341.
[75] P.D. Boyer, Current Topics in Bioenergetics 2 (1967) 99.
[76] E.C. Slater, Quart. Rev. Biophys. 4 (1971) 35.
[77] R.A. Morton, ed., Biochemistry of Quinones (Academic Press, New York, 1965).
[78] D.F. Wilson, M. Erecinska, P.L. Dutton and T. Tsudzuki, Biochem. Biophys. Res. Commun. 41 (1970) 1273.
[79] M. Erecinska, D.F. Wilson, Y. Mukai and B. Chance, Biochem. Biophys. Res. Commun. 41 (1970) 386.
[80] D.F. Wilson, Discussion, Second Symposium on Oxidases and Related Redox Systems, eds. T.E. King, H.S. Mason and M. Morrison (John Wiley, New York) in press.
[81] A. Boveris, R. Oshino, M. Erecinska and B. Chance, Biochim. Biophys. Acta 245 (1971) 1.
[82] F.J. Ruzicka and F.L. Crane, Biochim. Biophys. Acta 223 (1971) 71.
[83] B. Chance, in: Blood Cells and Plasma Proteins, ed. J.L. Tullis (Academic Press, New York, 1953) p. 306.
[84] J. Beetlestone, Arch. Biochem. Biophys. 89 (1960) 35.
[85] I. Pecht, Proc. Natl. Acad. Sci. U.S. 69 (1972) 902.
[86] K. Wüttrich, Proc. Natl. Acad. Sci. U.S. 63 (1969) 1071.
[87] A. Azzi, A. Tumburro and E. Sobbi, Biochim. Biophys. Acta, in press.
[88] H. Drott, C.P. Lee and T. Yonetani, J. Biol. Chem. 245 (1970) 5875.
[89] C.D. Frye and J. Ediden, J. Cell. Sci. 7 (1970) 313.
[90] S.J. Singer and G.L. Nicholson, Science 175 (1972) 720.
[91] B. Chance, in: Oxidases and Related Redox Systems, eds. T.E. King, H.S. Mason and M. Morrison (John

Wiley, New York, 1965) p. 929.
[92] H. Wohlrab, Biochemistry 9 (1970) 474.
[93] W.F. Holmes, Dissertation, The Rate Law of Interaction between Bound Chemicals, University of Pennsylvania, 1964.
[94] B. Chance, Federation Proc. 29 (1970) 735.
[95] P.K. Brown, Nature New Biol. 236 (1972) 35.
[96] R.A. Cone, Nature New Biol. 236 (1972) 39.
[97] R.E. Dickerson, Scientific American (1972) 226.
[98] H. Kimelberg and C.P. Lee, J. Mol. Biol. 2 (1970) 252.
[99] B. Chance, C.P. Lee, A. Waggoner, S. Papa and G.K. Radda, Abstracts, 11th Annual Biophysical Society Mtg., 1971, WPM-A-16.
[100] B. Chance, in: Proceedings, Intern. Congr. on the Biochemistry and Biophysics of Mitochondrial Membranes (Bressanone, Italy, 1971) in press.
[101] J. Cain, G. Santillan and J.K. Blasie, in: Membrane Research (Proceedings, ICN-UCLA Symp. Molecular Biology) ed. C. Fred. Fox (Academic Press, New York) in press.
[102] H.P. Ting, D.F. Wilson and B. Chance, Arch. Biochem. Biophys. 141 (1970) 141.
[103] R.J. Fisher, J.C. Chen, B.P. Sani, S.S. Kaplay and D.R. Sanadi, Proc. Natl. Acad. Sci. U.S. 68 (1971) 2184.
[104] P. Mitchell, Chemiosmotic Coupling and Energy Transduction (Glynn Res. Ltd., Bodmin, England, 1968).
[105] K.A. Davis and Y. Hatefi, Biochem. Biophys. Res. Commun. 44 (1971) 1338.
[106] B. Chance and G.R. Williams, Adv. Enzymol. 17 (1956) 65.
[107] J. Wang, Science 167 (1970) 25.
[108] P.D. Boyer, in: Oxidases and Related Redox Systems, eds. T.E. King, H.S. Mason and M. Morrison (John Wiley, New York, 1965) p. 994.
[109] B. Chance, C.P. Lee and L. Mela, Federation Proc. 26 (1967) 1341.
[110] B.T. Storey, J. Theoret. Biol. 31 (1970) 533.
[111] A. Jagendorf, in: Progress in Photosynthesis Research, II (Proceedings, 2nd Intern. Conf. on Photosynthesis, Stresa, Italy, 1971) in press.

Notes added in proof:

a) Davis et al. report that succinate–cytochrome-*c* reductase (complex-III) contains *both* cytochromes b_K and b_T, as well as cytochrome c_1.
K.A. Davis, K.L. Poff, W.L. Butler and Y. Hatefi, Federation Proc. 31 (1972) 853, Abs. 3611.

b) Duttoin reports that the mid-potential of cytochrome c_1 moves to 170 mV when that of cytochrome b_T is at 240 mV. International Conference on "Mechanisms in Bioenergetics", Pugnochioso, 1–4 May 1972.